

Spin Elastodynamic Motive Force

 Takumi Funato^{1,2} and Mamoru Matsuo^{2,3,4,5}
¹Center for Spintronics Research Network, Keio University, Yokohama 223-8522, Japan

²Kavli Institute for Theoretical Sciences, University of Chinese Academy of Sciences, Beijing 100190, China

³CAS Center for Excellence in Topological Quantum Computation, University of Chinese Academy of Sciences, Beijing 100190, China

⁴RIKEN Center for Emergent Matter Science (CEMS), Wako, Saitama 351-0198, Japan

⁵Advanced Science Research Center, Japan Atomic Energy Agency, Tokai 319-1195, Japan

 (Received 20 October 2021; revised 30 November 2021; accepted 20 January 2022; published 18 February 2022)

The spin-motive force (SMF) in a simple ferromagnetic monolayer caused by a surface acoustic wave is studied theoretically via spin-vorticity coupling (SVC). The SMF has two mechanisms. The first is the SVC-driven SMF, which produces the first harmonic electromotive force, and the second is the interplay between the SVC and the magnetoelastic coupling, which produces the dc and second harmonic electromotive forces. We show that these electric voltages induced by a Rayleigh-type surface acoustic wave can be detected in polycrystalline nickel. No sophisticated device structures, noncollinear magnetic structures, or strong spin-orbit materials are used in our approach. Consequently, it is intended to broaden the spectrum of SMF applications considerably.

DOI: 10.1103/PhysRevLett.128.077201

Introduction.—Spintronics is concerned with the interconversion of charge transport and spin dynamics. The use of charge current to control magnetization structures, such as magnetic domain walls, has been extensively investigated for spin-torque oscillators [1–3] and magnetoresistive random access memory applications [4–6]. The spin-transfer torque is a phenomenon where the orientation of the magnetization is controlled by injected spin-polarized current via the s-d coupling [7–9]. The spin-motive force (SMF), known as an inverse spin-transfer torque effect, is an electric voltage generation in a ferromagnetic metal due to an emergent spin-dependent gauge field driven by the interplay between conduction electron spins and the magnetization dynamics [10–13]. The first experiment involves observing the SMF in a nanowire due to magnetic domain wall motion [14–16].

The conventional SMF requires both nonvanishing time and space derivatives of the magnetization as $\mathbf{E}_{\text{con},i} \propto \mathbf{m} \cdot (\partial_t \mathbf{m} \times \partial_i \mathbf{m})$, where \mathbf{m} is the unit vector of the magnetization. Therefore, the latter requirement of the space derivative restricts the experimental setup. Indeed, the SMF induced by excited magnetization dynamics was measured in nonuniform magnetic textures formed by a comb-shaped device [17], the magnetic vortex on a gyrating disk [18], a wedged-shaped device [19], exchange-coupled ferromagnetic bilayers [20], and helical magnetism [21,22]. In an attempt to resolve the restriction, it is theoretically proposed that the SMF is induced via spin-orbit interaction, which does not require nonvanishing space derivative, e.g., the SMF induced by the oscillating magnetic field in systems with Rashba spin-orbit interaction [23] and time-varying gate voltage in systems with

strong spin-orbit interaction [24–27]. However, these mechanisms require strong spin-orbit materials, which means that they restrict the range of material choices.

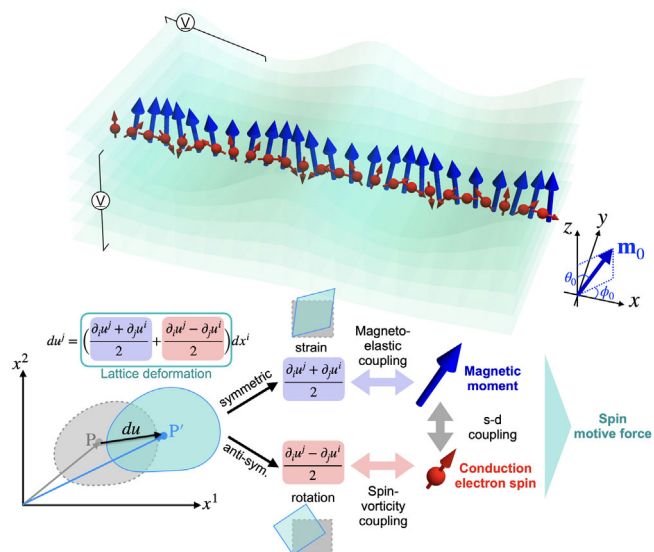


FIG. 1. Schematics of the mechanism of the spin elastodynamic motive force. In a ferromagnetic metal, the symmetric part of the deformation couples to magnetization (the magnetoelastic coupling) while the antisymmetric part couples to electron spin (the spin-vorticity coupling). When a surface acoustic wave is excited in the ferromagnet, these couplings generate two different spatially nonuniform spin dynamics of the magnetization and electron spins. With the s-d coupling between magnetization and spins, the unconventional spin motive force is induced. In particular, the spin-vorticity coupling allows the spin-motive force that does not rely on complicated structures and strong spin-orbit materials.

Accordingly, they have not been observed experimentally so far. As mentioned above, there is little variety in experimental reports on the SMFs because of experimental restrictions such as sophisticated device structures, noncollinear magnetic structures, and strong spin-orbit systems.

We propose the SMF induced by surface acoustic waves (SAWs) via spin elastodynamics to overcome conventional limitations. Three couplings drive the spin elastodynamics in a ferromagnetic metal: spin-vorticity coupling (SVC), magnetoelastic coupling, and s-d coupling (Fig. 1). In this setup, the injected SAW generates the magnetization dynamics with the nonvanishing time and space derivatives. The advantage of the SAW device is that it does not require nanofabrications of the magnetic metal itself, which are indispensable for the conventional SMF. We prepare, e.g., the interdigital transducers on the outside of the sample. In addition, the SVC, the coupling between conduction electron spins and the vorticity field of the lattice, emerges universally in various systems, and thus, it does not restrict material choices. Indeed, SVC has attracted much attention because it generates spin current without spin-orbit interaction. The spin current generated via SVC has been experimentally observed in spin-current generation by vortices associated with the liquid metal flow [28–32] and by vortex motion of lattice associated with SAWs [33–37]. The effective magnetic field owing to the rotational motion has been directly detected using NMR and NQR [38–44]. Also, magnetoelastic coupling has been widely exploited for driving nonequilibrium spin dynamics with a SAW [45,46]. In the presence of a SAW, the SVC, the coupling of electron spins and the vorticity of the lattice of the moving materials, plays a significant role in spin manipulations [47–53].

Because of the rotational motion of the lattice associated with the SAWs, the conduction electrons are subjected to SVC when they are applied to ferromagnetic metals. Through the s-d coupling, the conduction electron spins adiabatically follow the magnetization direction, and the SVC is modulated by the magnetization's precession motion, which causes the SMF. Simultaneously, the magnetoelastic coupling operates on the magnetization to excite the magnetization precession owing to lattice strain dynamics.

The current study finds a way to get over the SMF's conventional limitations. Thus, we concentrate on the SAW-induced SMF via SVC, a material-independent interaction [54]. We calculate the SAW-induced SMF up to second order in lattice displacement via treating the influence of magnetization dynamics as a unitary transformation of the spin space. The SAW-induced SMF has two mechanisms. The first, we call the SVC-driven SMF, produces an ac electromotive force oscillating at frequency ω of the SAW, which is induced by the gradient spin accumulation via the SVC. The second, we call the spin

elastodynamic motive force (SEMF), produces a dc electromotive force and an ac one oscillating at 2ω due to the interplay between the SVC acting on conduction electron spins and the magnetoelastic coupling acting on magnetization. The SEMF generates dc electromotive force in the film thickness direction when an out-of-plane magnetic field is applied. These findings show that the SEMF causes nonreciprocity of the electromotive force.

Model.—We consider the free-electron system coupled to the magnetization through the s-d coupling. The conduction electron's Lagrangian is expressed by

$$\mathcal{L} = \int_{x'} c_{x't}^{\dagger} \left[i\hbar\partial_t + \frac{\hbar^2}{2m} \nabla'^2 - V(x') - J_{sd} \mathbf{m}' \cdot \hat{\boldsymbol{\sigma}} \right] c_{x't}, \quad (1)$$

where $c_{x't}^{\dagger}$ and $c_{x't}$ are electron creation and annihilation operators, respectively, $\hat{\boldsymbol{\sigma}} = (\hat{\sigma}^x, \hat{\sigma}^y, \hat{\sigma}^z)$ are the Pauli matrices, \mathbf{m}' is the unit vector of the magnetization, J_{sd} is the exchange splitting constant, and V is the potential due to the lattice and impurities. When the lattice distortion dynamics are induced, the potentials are modulated as $V(\mathbf{x}' - \mathbf{u})$, where \mathbf{u} is the displacement vector of the lattice. Treating the lattice distortion effect, we perform the local coordinate transformation from the laboratory frame \mathbf{x}' to the rotating frame $\mathbf{x} = \mathbf{x}' - \mathbf{u}$. The conduction electron's Lagrangian is expressed as $\mathcal{L} = \mathcal{L}_0 + \mathcal{L}_{sv}$, where \mathcal{L}_0 is given by

$$\mathcal{L}_0 = \int_{\mathbf{x}} c_{x't}^{\dagger} \left[i\hbar\partial_t + \frac{\hbar^2}{2m} \nabla^2 - V(\mathbf{x}) - J_{sd} \mathbf{m} \cdot \hat{\boldsymbol{\sigma}} \right] c_{x't}, \quad (2)$$

where $c_{x't} = \sqrt{1 + \nabla \cdot \mathbf{u}} c_{x't}^{\prime}$ and $\mathbf{m}' = \mathcal{R}(r_{ij}) \mathbf{m}$ is the unit vector of the magnetization in the rotating frame with $\mathcal{R}(r_{ij})$ being the SO(3) rotation matrix and $r_{ij} = \frac{1}{2}(\partial_i u^j - \partial_j u^i)$ being the rotation tensor associated with the coordinate transformation. The \mathcal{L}_{sv} is the SVC:

$$\mathcal{L}_{sv} = \frac{\hbar}{4} \int_{\mathbf{x}} c_{x't}^{\dagger} \hat{\boldsymbol{\sigma}} \cdot \boldsymbol{\Omega} c_{x't}, \quad (3)$$

where $\boldsymbol{\Omega}_k = 2\epsilon_{ijk} \partial_i r_{ij}$ is the vorticity of the lattice motion. Note that the modulation of the kinetic energy and the time derivative appear; however, they are not dominant in this study and are neglected. We perform the rotational transformation in the spin space $c_{x't} = U(\mathbf{x}, t) a_{x't}$ with the direction of magnetization \mathbf{m} in the z direction, where $a_{x't}^{\dagger}$ and $a_{x't}$ are the electron creation and annihilation operators, respectively, after the rotational transformation. Here the unitary operator U is determined to satisfy $c^{\dagger} \mathbf{m} \cdot \hat{\boldsymbol{\sigma}} c = a^{\dagger} \hat{\sigma}^z a$. The conduction electron's Lagrangian including the SVC after the transformation is given by

$$\tilde{\mathcal{L}} = \int_{\mathbf{x}} a_{x't}^{\dagger} \left[i\hbar\partial_t - \frac{(\mathbf{p} + e\hat{\mathbf{A}}^s)^2}{2m} - \tilde{V} + e\hat{\mathbf{A}}_0^s - J_{ex} \sigma^z \right] a_{x't}, \quad (4)$$

where $\mathbf{p} = -i\hbar\nabla$ is the momentum operator and $\tilde{V} = U^\dagger V U$. Here, \hat{A}_0^s and \hat{A}^s are the effective spin scalar and vector potentials, given by $\hat{A}_0^s = (i\hbar/e)U^\dagger \partial_t U + (\hbar/4e)U^\dagger (\hat{\sigma} \cdot \boldsymbol{\Omega})U$, and $\hat{A}^s = -(i\hbar/e)U^\dagger \nabla U$. Particularly, the second term of \hat{A}_0^s is spin scalar potential induced by the SVC. The effective electric field is obtained by $\hat{\mathbf{E}}^s = -\partial_t \hat{A}^s - \nabla \hat{A}_0^s$. The total SMF is given by $\mathbf{E}_{\text{smf}} = P \text{tr}(\hat{\sigma}^z \hat{\mathbf{E}}^s)$, where P is the spin polarization of conduction electrons. The SAW-induced SMF contains two terms:

$$\mathbf{E}_{\text{smf}} = \mathbf{E}_{\text{con}} - \frac{P\hbar}{2e} \nabla(\mathbf{m} \cdot \boldsymbol{\Omega}), \quad (5)$$

where the first term $E_{\text{con},i} = (P\hbar/e)\mathbf{m} \cdot (\partial_t \mathbf{m} \times \partial_i \mathbf{m})$ is the conventional SMF, and the second term is the SMF induced via the SVC, which is dominant in this setup.

The spin dynamics generated by SAWs under a static magnetic field is determined by

$$\partial_t \mathbf{m}' = \gamma(\mathbf{h}_{\text{eff}} + \mathbf{h}_{\text{me}}) \times \mathbf{m}' - \alpha(\partial_t \mathbf{m}') \times \mathbf{m}', \quad (6)$$

where $\gamma(>0)$ is the gyromagnetic constant, α is the Gilbert damping constant, and \mathbf{h}_{eff} is a static effective magnetic field containing the static magnetic field and an anisotropy field. We assume that the Barnett field is negligible compared to the effective magnetic field due to the magnetoelastic coupling, which is given by [55]

$$h_{\text{me},i} = -\frac{2}{M_s} \sum_j e_{ij} m'_j [b_1 \delta_{ij} + b_2 (1 - \delta_{ij})], \quad (7)$$

where $e_{ij} = \frac{1}{2}(\partial_i u_j + \partial_j u_i)$ is the strain tensor, M_s is the saturation magnetization, and b_1 and b_2 are the magnetoelastic coupling constants. The magnetization processes around \mathbf{h}_{eff} with the resonance frequency of the Kittel modes ω_K in the spin-wave approximation. The magnetization vector in the rotating frame is given by $\mathbf{m} = \mathbf{m}_0 + \delta\mathbf{m} + \mathcal{O}(u^2)$, where $\mathbf{m}_0 = (\sin\theta_0 \cos\phi_0, \sin\theta_0 \sin\phi_0, \cos\theta_0)$ is the static component and $\delta\mathbf{m}$ is the dynamical component with θ_0 and ϕ_0 being shown in Fig. 1. Note that the magnetization modulation associated with the rotational transformation is negligible because of a higher order of Gilbert damping.

The lattice displacement \mathbf{u} with the Rayleigh-type SAW proceeding in the x direction is given by [56]

$$\mathbf{u} = u_0 e^{iq_\mu x^\mu} \begin{pmatrix} i\hat{s}_q \left(e^{\kappa_1 z} - \frac{2\kappa_1 \kappa_1}{\kappa_1^2 + q^2} e^{\kappa_1 z} \right) \\ 0 \\ \frac{\kappa_1}{|q|} \left(e^{\kappa_1 z} - \frac{2q^2}{\kappa_1^2 + q^2} e^{\kappa_1 z} \right) \end{pmatrix}, \quad (8)$$

where u_0 is the deformation amplitude of the SAW, \hat{s}_q is the sign function of q , and κ_1^{-1} and κ_1^{-1} are decay lengths of

longitudinal and transverse waves, respectively. Here, $q_\mu = (-\omega, \mathbf{q})$ are a frequency ω of the SAW and a wave number vector $\mathbf{q} = (q, 0, 0)$ of a longitudinal wave, and $x^\mu = (t, \mathbf{x})$ are time and coordinate. The vorticity $\boldsymbol{\Omega}$ is given by

$$\boldsymbol{\Omega}_y = \frac{2r_0\omega^2}{c_R} \hat{s}_q e^{\kappa_1 z} e^{iq_\mu x^\mu}, \quad (9)$$

where $c_R = \omega/|q|$ is a velocity of the SAW and $r_0 = |u_z(z=0)|$.

Results.—The SAW-induced SMFs contribute to the SMF because the conventional SMF, as is well known, turns out to vanish in the noncollinear magnetization structure. The SAW-induced SMF is given by up to second order in u .

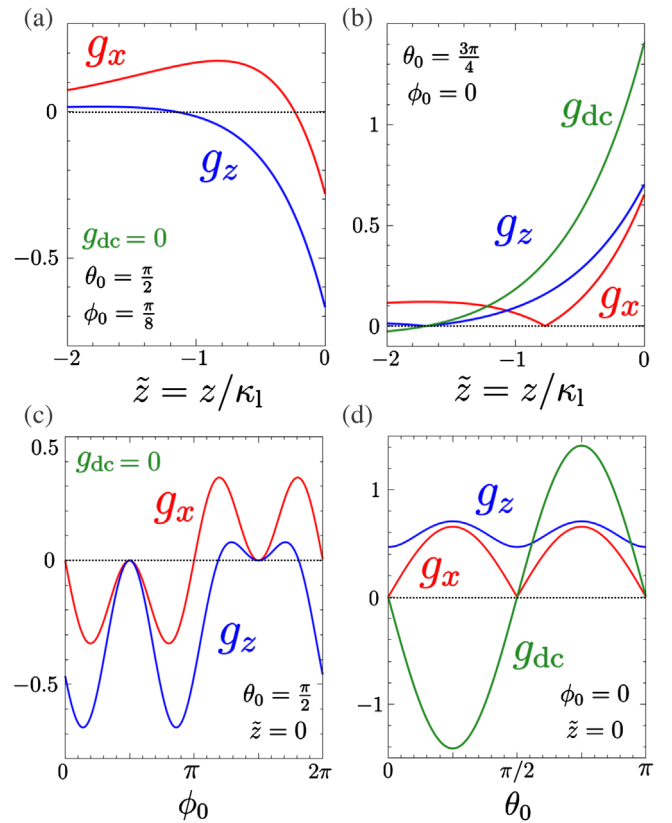


FIG. 2. The dependence of the SEMF on the depth from the surface (a),(b) and the direction of the applied magnetic field (c), (d). The red and blue lines represent the second harmonic component in the x direction and z direction, and the green lines represent the dc component in the z direction. The depth from the surface \tilde{z} is normalized by the decay constant of the longitudinal wave κ_1 . Here, we assume the isotropic system, and $b_1 = b_2$ is satisfied. (a) and (c) The case of an in-plane magnetic field applied ($\theta_0 = (\pi/2)$), and the dc component vanishes. (b) and (d) The case of an out-of-plane magnetic field applied ($\phi_0 = 0$), and both the second harmonic and dc components are induced. According to (c), the characteristic nonreciprocity is found in the z direction SMF.

TABLE I. The characteristics of the SVC-driven SMF and the SEMF, which do not require any device and material restrictions such as nonuniform device structure, noncollinear magnetization, and strong spin-orbit systems if only the SAW devices are available. MEC represents magnetoelastic coupling and IP and OP represent cases where the magnetic field is in the in-plane and out-of-plane directions. The SAW-induced SMFs produce various types of electromotive forces such as dc and ac oscillating at ω and 2ω .

Mechanisms	Interaction	Device	IP ($\theta_0 = 0$)	OP ($\theta_0 \neq 0$)
SEMF	SVC, MEC	SAW device	2ω	dc, 2ω
SVC-driven SMF	SVC		ω	ω

$$\mathbf{E}_{\text{smf}} = \mathbf{E}_{\text{sv}} + \mathbf{E}_{\text{s-m}}. \quad (10)$$

The first term $\mathbf{E}_{\text{sv}} = -(\hbar/2e)\nabla(\mathbf{m}_0 \cdot \mathbf{\Omega})$ is the ac component oscillating at ω due to the gradient spin accumulation induced by the SVC, which we call SVC-driven SMF, given by

$$\begin{pmatrix} E_{\text{sv},x} \\ E_{\text{sv},z} \end{pmatrix}_{\omega} = \mathcal{E}_{\text{sv}} \sin \theta_0 \sin \phi_0 e^{\kappa_1 z} \begin{pmatrix} \sin(q_{\mu} x^{\mu}) \\ -\frac{\kappa_1}{|q|} \mathfrak{z}_q \cos(q_{\mu} x^{\mu}) \end{pmatrix}, \quad (11)$$

where $\mathcal{E}_{\text{sv}} = (P\hbar r_0/ec_R^2)\omega^3$ a function of ω with the dimension of an electric field. The second term in Eq. (10) is given by $\mathbf{E}_{\text{s-m}} = -(\hbar/2e)\nabla(\delta\mathbf{m} \cdot \mathbf{\Omega})$ from the combination of SVC and magnetoelastic coupling, which we call spin elastodynamic motive force (SEMF). The SEMF contains the second harmonic component oscillating at 2ω and dc component. The second harmonic component is given by

$$\begin{pmatrix} E_{\text{s-m},x} \\ E_{\text{s-m},z} \end{pmatrix}_{2\omega} = \mathcal{E}_{\text{s-m}} \mathfrak{z}_q \begin{pmatrix} g_x \sin(2q_{\mu} x^{\mu} + \mathfrak{z}_q \Theta_x) \\ g_z \cos(2q_{\mu} x^{\mu} + \mathfrak{z}_q \Theta_z) \end{pmatrix}, \quad (12)$$

and the dc component is given by

$$\begin{pmatrix} E_{\text{s-m},x} \\ E_{\text{s-m},z} \end{pmatrix}_{\text{dc}} = \mathcal{E}_{\text{s-m}} \mathfrak{z}_q \begin{pmatrix} 0 \\ g_{\text{dc}} \end{pmatrix}, \quad (13)$$

where $\mathcal{E}_{\text{s-m}} = (P\hbar\gamma b_1/2e\omega_K\alpha M_s)(u_0 r_0/c_R^3)\omega^4$ is the function of ω , and $g_{x/z}$, g_{dc} are dimensionless functions of z , θ_0 , ϕ_0 , and \mathfrak{z}_q . The dependence of the SEMF on the depth from the surface and direction of the applied magnetic field are shown in Fig. 2 (the detailed calculation can be found in the Supplemental Material [57]). According to Fig. 2(c), the second harmonic component on the z direction has characteristic nonreciprocity. This nonreciprocity originates from the magnetoelastic coupling, demonstrated in the context of the spin-wave excitation by SAWs [58–62]. It should be noted that neither the second harmonic generation nor nonreciprocity occurs in the conventional SMF. These features are caused by the interplay between the magnetoelastic coupling and the SVC. Note that $\Theta_{x/z}$ are

dimensionless functions representing phase shift and turn out to vanish in $\theta_0 = (\pi/2)$.

Discussion.—Let us estimate the magnitude of the SVC-driven SMF \mathcal{E}_{sv} and the SEMF $\mathcal{E}_{\text{s-m}}$ in polycrystalline nickel with strong magnetoelastic coupling. When the Rayleigh-type SAW with frequency $f = 10$ GHz is applied, SVC-driven SMF is estimated as $\mathcal{E}_{\text{sv}} \sim 5.01 \times 10^{-2}$ V/m, and SEMF is estimated as $\mathcal{E}_{\text{s-m}} \sim 5.25 \times 10^{-3}$ V/m. This estimation suggests that an observable voltage, about nV order, induced for a distance of about μm , which is comparable with the continuous generation of the conventional SMF [17]. Here, longitudinal wave velocity is $c_l = 6.04 \times 10^3$ m/s, transverse wave velocity is $c_t = 3.00 \times 10^3$ m/s [63], velocity of Rayleigh-type SAW is $c_R = 2.80 \times 10^3$ m/s [64], saturation magnetization is $M_s = 0.61$ T [65], damping constant is $\alpha = 4.5 \times 10^{-2}$ [66], gyromagnetic ratio is $\gamma = 2.41 \times 10^5$ mA $^{-1}$ s $^{-1}$ [67], magnetoelastic coupling constant is $b_1 = b_2 = 9.5$ MJ/m 3 , and lattice displacement is $u_0 = 3.5 \times 10^{-12}$ m, which is 1% of the nickel lattice constant.

Surprisingly, the current processes in typical ferromagnetic materials with simple structures, such as nickel, can induce the SMF. Complex device structures or noncollinear magnetization structures are required in conventional SMFs. A Rashba device with spatial inversion symmetry breaking, a gate voltage modulation, and a strong spin-orbit material are all material constraints for SMFs induced via spin-orbit interaction. Because there are no restrictions on device structures or materials, the SVC-driven SMF and the SEMF enable technical applications, such as microfabrication on magnetic materials. The SVC-driven SMF and the SEMF simultaneously generate the dc and ac components oscillating at ω and 2ω , and the current mechanisms are summarized in Table I.

Conclusion.—To address the limits of typical SMF processes, we theoretically analyzed the SMF induced by a Rayleigh-type SAW. We discovered two mechanisms of the SAW-induced SMF via the SVC. The first is the SVC-driven SMF, which generates the first harmonic electromotive force due to gradient spin accumulation induced by SVC, and the second is the SEMF, which generates dc and the second harmonic electromotive force due to the combination of SVC and magnetoelastic

coupling. Particularly, the dc SMF is induced under an applied out-of-plane magnetic field. The results suggest that the second harmonic component on the z direction has characteristic nonreciprocity. Our estimation suggests that the electric voltage induced by the present SMFs is detectable in polycrystalline nickel. The present SMFs can be generated in ferromagnet without restrictions on device structure or materials if only the SAW device is available. Therefore, the SVC-driven SMF and the SEMF are expected to expand the range of the SMF applications greatly. Furthermore, the present results may have implications for strain-related spintronics, e.g., the piezospintronic effect [68–70], flexible spintronics [71–73], and mechanical control of spin-orbit interaction [74,75].

We would like to thank Y. Nozaki, K. Yamanoi, T. Horaguchi, J. Fujimoto, and D. Oue for enlightening discussions. This work was partially supported by JST CREST Grant No. JPMJCR19J4, Japan. T. F. is supported by JSPS KAKENHI for Grants No. 21K20356. M. M. is supported by JSPS KAKENHI for Grants (No. 20H01863 and No. 21H04565) and the Priority Program of the Chinese Academy of Sciences, Grant No. XDB28000000.

-
- [1] S. I. Kiselev, J. C. Sankey, I. N. Krivorotov, N. C. Emley, R. J. Schoelkopf, R. A. Buhrman, and D. C. Ralph, *Nature (London)* **425**, 380 (2003).
- [2] W. H. Rippard, M. R. Pufall, S. Kaka, S. E. Russek, and T. J. Silva, *Phys. Rev. Lett.* **92**, 027201 (2004).
- [3] J. A. Katine and E. E. Fullerton, *J. Magn. Magn. Mater.* **320**, 1217 (2008).
- [4] M. Hosomi, H. Yamagishi, T. Yamamoto, K. Bessyo, Y. Higo, K. Yamane, H. Yamada, M. Shoji, H. Hachino, C. Fukumoto, H. Nagao, and H. Kano, *IEEE International Electron Devices Meeting, 2005* (IEEE, New York, 2005), 459, 10.1109/IEDM.2005.1609379.
- [5] S. Ikeda, J. Hayakawa, Y. M. Lee, F. Matsukura, Y. Ohno, T. Hanyu, and H. Ohno, *IEEE Trans. Electron Devices* **54**, 991 (2007).
- [6] S. Matsunaga, J. Hayakawa, S. Ikeda, K. Miura, H. Hasegawa, T. Endoh, H. Ohno, and T. Hanyu, *Appl. Phys. Express* **1**, 091301 (2008).
- [7] J. C. Slonczewski, *J. Magn. Magn. Mater.* **159**, L1 (1996).
- [8] L. Berger, *Phys. Rev. B* **54**, 9353 (1996).
- [9] J. A. Katine, F. J. Albert, R. A. Buhrman, E. B. Myers, and D. C. Ralph, *Phys. Rev. Lett.* **84**, 3149 (2000).
- [10] L. Berger, *Phys. Rev. B* **33**, 1572 (1986).
- [11] G. E. Volovik, *J. Phys. C* **20**, L83 (1987).
- [12] A. Stern, *Phys. Rev. Lett.* **68**, 1022 (1992).
- [13] S. E. Barnes and S. Maekawa, *Phys. Rev. Lett.* **98**, 246601 (2007).
- [14] S. A. Yang, G. S. D. Beach, C. Knutson, D. Xiao, Q. Niu, M. Tsoi, and J. L. Erskine, *Phys. Rev. Lett.* **102**, 067201 (2009).
- [15] S. A. Yang, G. S. D. Beach, C. Knutson, D. Xiao, Z. Zhang, M. Tsoi, Q. Niu, A. H. MacDonald, and J. L. Erskine, *Phys. Rev. B* **82**, 054410 (2010).
- [16] M. Hayashi, J. Ieda, Y. Yamane, J.-i. Ohe, Y. K. Takahashi, S. Mitani, and S. Maekawa, *Phys. Rev. Lett.* **108**, 147202 (2012).
- [17] Y. Yamane, K. Sasage, T. An, K. Harii, J. Ohe, J. Ieda, S. E. Barnes, E. Saitoh, and S. Maekawa, *Phys. Rev. Lett.* **107**, 236602 (2011).
- [18] K. Tanabe, D. Chiba, J. Ohe, S. Kasai, H. Kohno, S. E. Barnes, S. Maekawa, K. Kobayashi, and T. Ono, *Nat. Commun.* **3**, 845 (2012).
- [19] M. Nagata, T. Moriyama, K. Tanabe, K. Tanaka, D. Chiba, J.-i. Ohe, Y. Hisamatsu, T. Niizeki, H. Yanagihara, E. Kita, and T. Ono, *Appl. Phys. Express* **8**, 123001 (2015).
- [20] W. Zhou, T. Seki, H. Imamura, J. Ieda, and K. Takanashi, *Phys. Rev. B* **100**, 094424 (2019).
- [21] N. Nagaosa, *Jpn. J. Appl. Phys.* **58**, 120909 (2019).
- [22] T. Yokouchi, F. Kagawa, M. Hirschberger, Y. Otani, N. Nagaosa, and Y. Tokura, *Nature (London)* **586**, 232 (2020).
- [23] K.-W. Kim, J.-H. Moon, K.-J. Lee, and H.-W. Lee, *Phys. Rev. Lett.* **108**, 217202 (2012).
- [24] C. S. Ho, M. B. A. Jalil, and S. G. Tan, *J. Appl. Phys.* **111**, 07C327 (2012).
- [25] C. S. Ho, M. B. A. Jalil, and S. G. Tan, *J. Appl. Phys.* **115**, 183705 (2014).
- [26] C. S. Ho, M. B. A. Jalil, and S. G. Tan, *New J. Phys.* **17**, 123005 (2015).
- [27] Y. Yamane, J. Ieda, and S. Maekawa, *Phys. Rev. B* **88**, 014430 (2013).
- [28] R. Takahashi, M. Matsuo, M. Ono, K. Harii, H. Chudo, S. Okayasu, J. Ieda, S. Takahashi, S. Maekawa, and E. Saitoh, *Nat. Phys.* **12**, 52 (2016).
- [29] R. Takahashi, H. Chudo, M. Matsuo, K. Harii, Y. Ohnuma, S. Maekawa, and E. Saitoh, *Nat. Commun.* **11**, 3009 (2020).
- [30] H. Tabaei Kazerooni, A. Thieme, J. Schumacher, and C. Cierpka, *Phys. Rev. Applied* **14**, 014002 (2020).
- [31] H. Tabaei Kazerooni, G. Zinchenko, J. Schumacher, and C. Cierpka, *Phys. Rev. Fluids* **6**, 043703 (2021).
- [32] M. Matsuo, Y. Ohnuma, and S. Maekawa, *Phys. Rev. B* **96**, 020401(R) (2017).
- [33] D. Kobayashi, T. Yoshikawa, M. Matsuo, R. Iguchi, S. Maekawa, E. Saitoh, and Y. Nozaki, *Phys. Rev. Lett.* **119**, 077202 (2017).
- [34] Y. Kurimune, M. Matsuo, S. Maekawa, and Y. Nozaki, *Phys. Rev. B* **102**, 174413 (2020).
- [35] Y. Kurimune, M. Matsuo, and Y. Nozaki, *Phys. Rev. Lett.* **124**, 217205 (2020).
- [36] S. Tateno, G. Okano, M. Matsuo, and Y. Nozaki, *Phys. Rev. B* **102**, 104406 (2020).
- [37] S. Tateno, Y. Kurimune, M. Matsuo, K. Yamanoi, and Y. Nozaki, *Phys. Rev. B* **104**, L020404 (2021).
- [38] H. Chudo, M. Ono, K. Harii, M. Matsuo, J. Ieda, R. Haruki, S. Okayasu, S. Maekawa, H. Yasuoka, and E. Saitoh, *Appl. Phys. Express* **7**, 063004 (2014).
- [39] H. Chudo, K. Harii, M. Matsuo, J. Ieda, M. Ono, S. Maekawa, and E. Saitoh, *J. Phys. Soc. Jpn.* **84**, 043601 (2015).
- [40] K. Harii, H. Chudo, M. Ono, M. Matsuo, J. Ieda, S. Okayasu, S. Maekawa, and E. Saitoh, *Jpn. J. Appl. Phys.* **54**, 050302 (2015).

- [41] M. Ono, H. Chudo, K. Harii, S. Okayasu, M. Matsuo, J. Ieda, R. Takahashi, S. Maekawa, and E. Saitoh, *Phys. Rev. B* **92**, 174424 (2015).
- [42] M. Arabgol and T. Sleanor, *Phys. Rev. Lett.* **122**, 177202 (2019).
- [43] H. Chudo, M. Imai, M. Matsuo, S. Maekawa, and E. Saitoh, *J. Phys. Soc. Jpn.* **90**, 081003 (2021).
- [44] H. Chudo, M. Matsuo, S. Maekawa, and E. Saitoh, *Phys. Rev. B* **103**, 174308 (2021).
- [45] M. Weiler, H. Huebl, F. S. Goerg, F. D. Czeschka, R. Gross, and S. T. B. Goennenwein, *Phys. Rev. Lett.* **108**, 176601 (2012).
- [46] L. Dreher, M. Weiler, M. Pernpeintner, H. Huebl, R. Gross, M. S. Brandt, and S. T. B. Goennenwein, *Phys. Rev. B* **86**, 134415 (2012).
- [47] M. Matsuo, J. Ieda, E. Saitoh, and S. Maekawa, *Phys. Rev. Lett.* **106**, 076601 (2011).
- [48] M. Matsuo, J. Ieda, E. Saitoh, and S. Maekawa, *Phys. Rev. B* **84**, 104410 (2011).
- [49] M. Matsuo, J. Ieda, E. Saitoh, and S. Maekawa, *Appl. Phys. Lett.* **98**, 242501 (2011).
- [50] M. Matsuo, J. Ieda, and S. Maekawa, *Phys. Rev. B* **87**, 115301 (2013).
- [51] M. Matsuo, J. Ieda, K. Harii, E. Saitoh, and S. Maekawa, *Phys. Rev. B* **87**, 180402(R) (2013).
- [52] M. Matsuo, J. Ieda, and S. Maekawa, *Solid State Commun.* **198**, 57 (2014).
- [53] M. Matsuo, E. Saitoh, and S. Maekawa, *J. Phys. Soc. Jpn.* **86**, 011011 (2017).
- [54] The material dependence of the SVC has not been reported experimentally: Y. Kurimune, M. Matsuo, S. Maekawa, and Y. Nozaki, *Phys. Rev. B* **102**, 174413 (2020); while the renormalization of the SVC due to material dependent effects is proposed theoretically: M. Matsuo *et al.*, *Phys. Rev. B* **87**, 115301 (2013).
- [55] S. Chikazumi, *Physics of Ferromagnetism*, 2nd ed. (Oxford University, Oxford, UK, 1987).
- [56] A. N. Cleland, *Foundation of Nanomechanics: From Solid-State Theory to Device Applications* (Springer, Berlin, 2003).
- [57] See Supplemental Material at <http://link.aps.org/supplemental/10.1103/PhysRevLett.128.077201> for detailed calculations.
- [58] R. Sasaki, Y. Nii, Y. Iguchi, and Y. Onose, *Phys. Rev. B* **95**, 020407(R) (2017).
- [59] M. Xu, J. Puebla, F. Auvray, B. Rana, K. Kondou, and Y. Otani, *Phys. Rev. B* **97**, 180301(R) (2018).
- [60] S. Tateno and Y. Nozaki, *Phys. Rev. Applied* **13**, 034074 (2020).
- [61] J. Puebla, M. Xu, B. Rana, K. Yamamoto, S. Maekawa, and Y. Otani, *J. Phys. D* **53**, 264002 (2020).
- [62] M. Xu, K. Yamamoto, J. Puebla, K. Baumgaertl, B. Rana, K. Miura, H. Takahashi, D. Grundler, S. Maekawa, and Y. Otani, *Sci. Adv.* **6**, 1724 (2020).
- [63] Chronological Scientific Tables 2021, edited by National Astronomical Observatory of Japan (Maruzen Publishing Co., Ltd., Tokyo, 2021) [in Japanese].
- [64] L. D. Landau, L. P. Pitaevskii, A. M. Kosevich, and E. M. Lifshitz, *Theory of Elasticity: Third Edition* (Butterworth-Heinemann, Oxford, 1986).
- [65] C. Seberino and H. Bertram, *IEEE Trans. Magn.* **33**, 3055 (1997).
- [66] J. Walowski, M. D. Kaufmann, B. Lenk, C. Hamann, J. McCord, and M. Münzenberg, *J. Phys. D* **41**, 164016 (2008).
- [67] A. J. P. Meyer and G. Asch, *J. Appl. Phys.* **32**, S330 (1961).
- [68] A. S. Núñez, *Solid State Commun.* **198**, 18 (2014).
- [69] C. Ulloa, R. E. Troncoso, S. A. Bender, R. A. Duine, and A. S. Nunez, *Phys. Rev. B* **96**, 104419 (2017).
- [70] Z. Liu, Z. Feng, H. Yan, X. Wang, X. Zhou, P. Qin, H. Guo, R. Yu, and C. Jiang, *Adv. Electron. Mater.* **5**, 1900176 (2019).
- [71] Y.-f. Chen, Y. Mei, R. Kaltofen, J. I. Mnch, J. Schumann, J. Freudenberger, H.-J. Klau, and O. G. Schmidt, *Adv. Mater.* **20**, 3224 (2008).
- [72] C. Barraud, C. Deranlot, P. Seneora), R. Mattanab), B. Dlubak, S. Fusil, K. Bouzehouane, D. Deneuve, F. Petroff, and A. Fert, *Appl. Phys. Lett.* **96**, 072502 (2010).
- [73] S. Ota, P. V. Thach, H. Awano, A. Ando, K. Toyoki, Y. Kotani, T. Nakamura, T. Koyama, and D. Chiba, *Sci. Rep.* **11**, 6237 (2021).
- [74] V. Sih, H. Knotz, J. Stephens, V. R. Horowitz, A. C. Gossard, and D. D. Awschalom, *Phys. Rev. B* **73**, 241316(R) (2006).
- [75] H. Sanada, T. Sogawa, H. Gotoh, K. Onomitsu, M. Kohda, J. Nitta, and P. V. Santos, *Phys. Rev. Lett.* **106**, 216602 (2011).